

An optimal design algorithm for centrifugal fans: Theoretical and experimental studies[†]

Cheng-Hung Huang^{*} and Min-Hsiang Hung

Department of Systems and Naval Mechatronic Engineering, National Cheng Kung University, Tainan, Taiwan, R.O.C.

(Manuscript Received January 2, 2012; Revised August 31, 2012; Accepted September 24, 2012)

Abstract

This study examines the inverse design problem (IDP) of determining the optimal three-dimensional shape of a centrifugal-flow fan based on a desired airflow rate. The desired volume airflow rate can be obtained by multiplying the airflow rate of an existing fan by a constant greater than unity. The geometry of the redesigned fan is generated using several design variables, which enables the shape of the fan to be constructed completely; thus, the parameter estimation technique used in inverse design problems can be used. Finally, prototypes of the original and optimized centrifugal fans are fabricated, and the fan performance is tested based on the AMCA-210-85 standard, which uses calibrated nozzles and pressure taps within a standardized test chamber, to verify the validity of this work. The experimental results demonstrate that by using the fabricated optimal fan, the airflow rate can be increased by 11.8 % and the fan noise can be reduced by 3.5 %; as a result, the performance of optimal fan is greatly improved.

Keywords: Inverse design problem; Centrifugal-flow fan; Optimal design problem; Levenberg-Marquardt method

1. Introduction

With their compact structures, centrifugal fans are applied widely to cool electronic devices, especially notebook computers. It is therefore important to improve their airflow rate and efficiency by redesigning the shape. Because of the variety of centrifugal fan applications, the shape design is an important issue for manufacturers, and they must develop their design technology effectively and efficiently. The analysis (or direct) problem of fans needs be performed repeatedly in the traditional design algorithms by modifying the design variables; therefore, it depends strongly on the designer's skills and experiences and requires much trial and error time to obtain the good design of the fan shapes. The pre-calculation process is particularly difficult and time-consuming, and this has gradually become a bottleneck in fan shape design.

At present, the rapid development of computational fluid dynamics has provided a strong research method for fan design optimization. General-purpose CFD packages have become highly professional and are widely used in engineering; increasingly, they play an important role in saving money and shortening the development cycle [1], thereby increasing efficiency.

Unlike traditional design methods, the inverse design

method provides an efficient algorithm for the optimization of fan shapes that meet operational requirements and specified constraints with minimal effort [2-4], thereby reducing the time used in design modification.

Direct problems associated with fan design include the determination of air velocity, airflow rate, pressure distribution and fan efficiency given specified operational conditions, system parameters and fan shape. In contrast, the inverse problem associated with centrifugal fan design considered in this work involves the determination of the optimal shape of centrifugal fans based on desired airflow rates.

Several studies on this topic can be found in the literature. Huang and Hsieh [5] numerically simulated backward-curved airfoil centrifugal blowers and compared the results with experimental data. The results show that the optimized design demonstrated a 7.9% improvement in static pressure and a 1.5% improvement in efficiency. A design of experiments (DOE) has been performed by Behzadmehr et al. [6] to study the effect of the entrance conditions of a backward-inclined centrifugal fan on its efficiency. The methodology employed was validated by comparing the predicted results from the DOE with the results of numerical simulations of the corresponding fan. Gardow [7] measured the velocities at the rotor inlet of a centrifugal fan, and the results indicated that the flow near the shroud was nearly axial and slowly changed to a radial flow at the back plate.

Lin and Huang [9] successfully designed a centrifugal fan to

^{*}Corresponding author. Tel.: +82 6 274 7018, Fax.: +82 6 274 7019

E-mail address: chhuang@mail.ncku.edu.tw

[†]Recommended by Associate Editor Gang-Won Jang

© KSME & Springer 2013

meet the cooling requirement of a notebook computer. They concluded that blade shapes will affect the passages between blades and that the airfoil blade can reduce the recirculation of flow on the blade suction surface, which is the major source of noise. Nevertheless, in the fan design studied by these authors, strong flow separation was observed at the blade inlet and identified as the major cause of flow rate reduction. They attributed this flow separation to the high-angle-attack of incoming flow and suggested aligning the blade with the inlet flow by changing the inlet angle of the blade. However, these authors did not provide the algorithm used to obtain the optimal shape of the airfoil blade and the optimal blade inlet angle.

One feature of centrifugal fan shape design problems is that they require complete regeneration of the mesh in the flow field as the fan geometry evolves, which leads to tedious re-meshing of the computational domain; for this reason, these problems are often classified as highly ill-posed. Therefore, an appropriate numerical method or an efficient method is required to solve this feature of the problem. The general purpose commercial code CFD-ACE+ [10] is adopted in the present work as the solution for three-dimensional Reynolds-averaged Navier-Stokes equations with the standard k - ϵ turbulence model.

An important first step in the proper formulation of the problem is to identify the design variables for the fan. If proper variables are not selected, the formulation will either be incorrect or impossible. At the initial stage of problem formulation, all possible design variables should be investigated. It is sometimes desirable to designate more design variables than may be apparent from the problem in the initial stage; later, it is possible to assign a fixed numerical value to any variable and thereby eliminate it from the problem formulation [11].

A four-digit-NACA airfoil NACA-mpta is used as the initial design for a fan blade, and the design variables are chosen as the blade section parameters; for NACA4412, the blade section parameters are 4 (m), 4 (p) and 12 (ta) three variables. The remaining system parameters are the outer radius of the impeller (r_2), the inner radius of the impeller (r_1), the width of the impeller (h), the radius of the rotor (R_h), the blade inlet angle (β), the number of blades (N), the inclined angle of the volute tongue (θ), the impeller blade-tongue clearance (Δr) and the radius of the inlet flow (R_i). The computation time for this fan shape design problem depends strongly on the number of design variables studied. Therefore, the design variables should be selected appropriately. Essentially, design variables that have a strong effect on fan performance should be selected. For this reason, these design variables should be subjected to sensitivity analysis to determine the critical design variables for use in the present inverse design problem.

The Levenberg-Marquardt method [12] has proven to be a powerful algorithm in inverse design calculations. It has been applied by Huang et al. [13] to predict the form of a ship's hull in accordance with the desired hull pressure distribution. Subsequently, Chen and Huang [14] applied the LMM to predict an unknown hull form based on the preferable wake distribu-

tion in the propeller disk plane. Chen et al. [15] also applied the LMM to the optimal design of a bulbous bow. Moreover, Huang and Chen [16] and Huang and Lin [17] applied a similar technique to design the shape of a gas channel for a proton exchange membrane fuel cell.

For this reason, we used the Levenberg-Marquardt method in this work to estimate an optimal fan geometry that satisfies the desired (or optimal) airflow rate. Finally, experiments are conducted based on the original and optimal fan shapes to compare the numerical and experimental results.

In section 2, the algorithm used to calculate the flow condition for a centrifugal fan (i.e., the direct problem) is explained. The design variables and the procedure used to generate the shape of fan are given in section 3. The shape design problem, including the sensitivity analysis of the design parameters and the definition of the cost function, and the Levenberg-Marquardt algorithm are addressed in section 4, and the optimization procedure is summarized in section 5. section 6 illustrates the equations that are used for statistical analysis, and the experiment used to test fan performance is addressed in section 7. Finally, the results are presented and discussed in section 8.

2. The direct problem

In the numerical computation of the flow field of a centrifugal fan, the three-dimensional motion of the gas is thought to be an incompressible and unsteady flow and is calculated using three-dimensional Reynolds Navier-Stokes equations. The flow is turbulent; thus, the standard k - ϵ equation of the second model was selected for turbulence modeling, and the standard wall function was used near the wall [18]:

$$\frac{\partial u_i}{\partial x_i} = 0 \quad (1)$$

$$\begin{aligned} & \frac{\partial}{\partial t}(\rho u_i) + \frac{\partial}{\partial x_i}(\rho u_i u_j) \\ &= -\frac{\partial p}{\partial x_i} + \frac{1}{3}\mu \frac{\partial}{\partial x_i} \left(\frac{\partial u_j}{\partial x_j} \right) + \mu \frac{\partial^2 u_i}{\partial x_j \partial x_j} \end{aligned} \quad (2)$$

$$\frac{D\epsilon}{Dt} = \frac{\partial}{\partial x_j} \left\{ \left[\mu + \frac{C_\mu \left(\frac{k^2}{\epsilon} \right)}{\sigma_k} \right] \frac{\partial k}{\partial x_j} \right\} + G_k - \epsilon \quad (3)$$

$$\frac{Dk}{Dt} = \frac{\partial}{\partial x_j} \left\{ \left[\mu + \frac{C_\mu \left(\frac{k^2}{\epsilon} \right)}{\sigma_\epsilon} \right] \frac{\partial \epsilon}{\partial x_j} \right\} + C_{\epsilon 1} \frac{\epsilon}{k} G_k - C_{\epsilon 2} \frac{\epsilon^2}{k} \quad (4)$$

The boundary type of the model inlet was set to velocity-inlet and turbulence intensity. The outlet type was set to pressure-outlet. The impeller selects the rotating coordinate, and the volute selects the still coordinate.

In this study, all of the above continuity and momentum equations for unsteady turbulent flow using the standard k - ϵ model are solved by using a general purpose computational

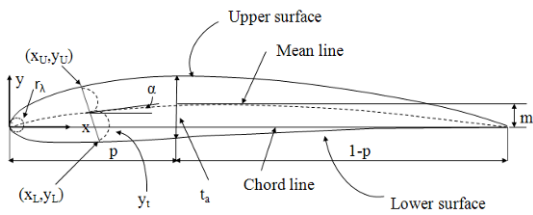


Fig. 1. The geometric parameters of a two-dimensional NACA blade section.

fluid dynamic code, CFD-ACE+, which employs a finite volume method, because CFD-ACE+ has the ability to handle the moving grid problem using the embedded “grid deformation” function.

The “moving grid problem” actually implies that the grids along the blade edge and the new fan shape can be fitted well with the grids in the flow field when the blades are rotating. In addition, the coupled set of equations needs be solved iteratively; the solution is considered convergent when the relative error in the flow field between consecutive iterations is less than a specified small number. Finally, the volume flow rate of the specific centrifugal fan can be calculated.

3. Fan shape generation

The following twelve variables can be adopted to generalize the initial shape of a centrifugal fan. For a four-digit-NACA airfoil NACA-mpta, the blade section parameters are (m , p , t_a) three variables, the outer radius of the impeller (r_2), the inner radius of the impeller (r_1), the width of the impeller (h), the radius of the rotor (R_h), the blade inlet angle (β), the number of blades (N), the inclined angle of the volute tongue (θ), the impeller blade-tongue clearance (Δr) and the radius of the inlet flow (R_i). The cross-sectional view of the NACA fan blade in terms of m , p and t_a is shown in Fig. 1, and the remaining variables for a centrifugal fan are shown in Fig. 2.

The method used to generate the shape of a centrifugal fan using the commercial software CFD-ACE+ can be summarized as follows: First, the cross-sectional data for the blade can be obtained using the formula for a four-digit-NACA airfoil and saved using a specified type file name, and a single blade can be mounted on the hub. The remaining fan blades can be duplicated by executing the rotation function in the CFD code to obtain the complete set of blades.

This file is imported into CFD, and the values for the outer radius of the impeller, the inner radius of the impeller, the width of the impeller, the radius of the rotor, the blade inlet angle, the number of blades, the inclined angle of the volute tongue, the impeller blade-tongue clearance and the radius of inlet flow are input. From these data, the shape of the complete centrifugal fan can be obtained by using the embedded function in CFD.

The preceding method of generating the geometry of a centrifugal fan can be saved by using a python-type file name. To obtain a new complete centrifugal fan, the above twelve de-

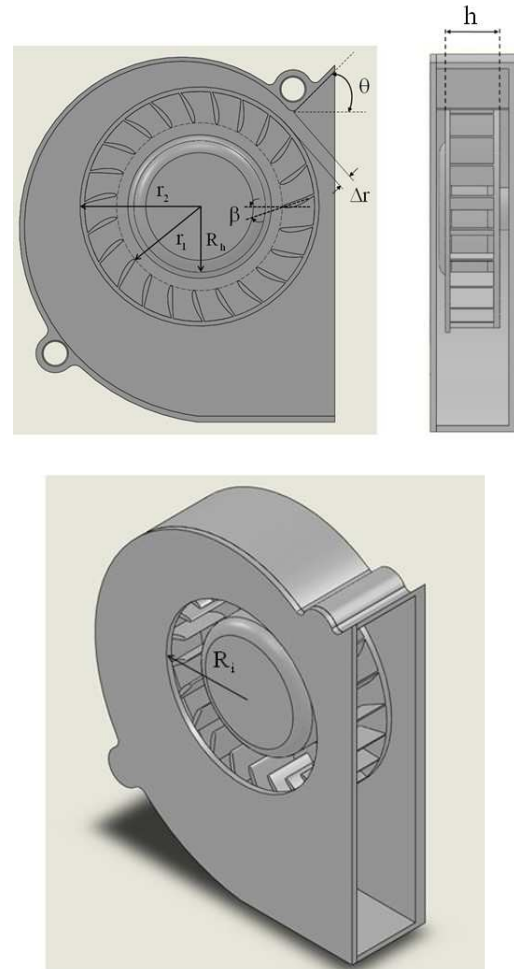


Fig. 2. The system variables of a centrifugal fan.

sign variables are simply input again, and the python file is re-executed. This simple centrifugal fan generation process solves the fan shape design problem neatly and efficiently.

4. The shape design problem using the Levenberg-Marquardt method(LMV)

4.1 The shape design problem

For the centrifugal fan shape design problem considered here, the desired but unknown new shape is controlled by a set of fan design variables. The desired volume flow rate of air is also considered a given parameter.

If the dimensions for the impeller and the volute are fixed, the fan variables r_1 , r_2 , h , N , α , and Δr are fixed, and the set of fan design variables is reduced to the six parameters m , p , t_a , R_h , β , and R_i .

If the fan design variables and desired volume flow rate of air are denoted by B_j and Θ , respectively, the inverse geometry design problem can be stated as follows: utilizing the desired volume flow rate of air, Θ , design the new shape for a centrifugal fan, Ψ . The desired volume flow rate of air, Θ , is always at zero static pressure, i.e., $P_s = 0$.

The solution of the centrifugal fan design problem is obtained in such a way that the following functional is minimized:

$$J[\Psi(B_j)] = \{Q[\Psi(B_j)] - \Theta\}^2 = U^T U ; j = 1 \text{ to } P . \quad (5)$$

Here, B_j , where $j = 1$ to P , represents the set of design variables, i.e.,

$$B_j = \mathbf{B} = \{B_1, B_2, B_3, B_4, B_5, B_6\} \\ = \{m, p, ta, R_h, \beta, R_i\}, \quad (6)$$

and $Q[\Psi(B_j)]$ represents the estimated or computed volume flow rate of air at $P_s = 0$.

This quantity is determined from the solution of the direct problem given previously with an estimated fan shape $\Psi(B_j)$ with design variables B_j . If the estimated volume flow rate of air Q is sufficiently close to the desired volume flow rate of air Θ , the corresponding estimated centrifugal fan shape $\Psi(B_j)$ can be regarded as the optimal shape of the redesigned centrifugal fan.

As previously mentioned, it is important to identify the proper design variables for the centrifugal fan in this design problem. In the initial stage of design, it is desirable to include more design variables than may be apparent from the problem; later, it is possible to assign a fixed numerical value to any variable and eliminate it from the problem formulation. For this purpose, the following sensitivity analysis of the design variables will be performed; then, only the most important design variables will be selected to reduce the computational time.

The effects of the design variables on the air volume flow rate are determined by perturbing the design variables B_j one at a time by $\pm 5\%$ of the original value (for m , p and ta , we used $\pm 1\%$). Then, we compute the resulting changes in the volume flow rate of air using Eqs. (1)-(4), i.e., the solution of the direct problem. If the changes in airflow rate are small for some design variables, these design variables are not sensitive to the design and can fixed at particular values.

4.2 The Levenberg-Marquardt method

The next step in the analysis is the minimization of the least squares equation, Eq. (5), by differentiating it with respect to each of the unknown design variables in the set B_j . If P design variables are used, Eq. (5) is minimized with respect to the set of design variables B_j and the resulting expression can then be set equal to zero. The following equation can be obtained:

$$\frac{\partial J[\Psi(B_j)]}{\partial B_j} = \left\{ \frac{\partial Q[\Psi(B_j)]}{\partial B_j} \right\} [Q - \Theta] = 0 ; j = 1 \text{ to } P . \quad (7)$$

Eq. (7) is linearized by expanding $Q[\Psi(B_j)]$ in a Taylor series and retaining the first-order terms. A damping parameter μ_n is added to the resulting expression to improve convergence. This will finally lead to the Levenberg-Marquardt method (LMM) [12] and is given by

ter μ_n is added to the resulting expression to improve convergence. This will finally lead to the Levenberg-Marquardt method (LMM) [12] and is given by

$$(\mathbf{F} + \mu^n \mathbf{I}) \Delta \mathbf{B} = \mathbf{D} \quad (8)$$

where

$$\mathbf{F} = \mathfrak{g}^T \mathfrak{g} \quad (9)$$

$$\mathbf{D} = \mathfrak{g}^T \mathbf{U} \quad (10)$$

$$\Delta \mathbf{B} = \mathbf{B}^{n+1} - \mathbf{B}^n . \quad (11)$$

Here, the superscripts n and T represent the iteration index and transpose matrix, respectively, \mathbf{I} is the identity matrix and \mathfrak{g} denotes the Jacobian matrix defined as

$$\mathfrak{g} = \frac{\partial Q}{\partial \mathbf{B}^T} . \quad (12)$$

The Jacobian matrix defined by Eq. (12) is determined by perturbing the unknown parameters B_j one at a time and computing the resulting change in the volume flow rate of air from the solution of the direct problem.

Eq. (8) is now written in a form that is suitable for iterative calculation:

$$\mathbf{B}^{n+1} = \mathbf{B}^n + (\mathfrak{g}^T \mathfrak{g} + \mu^n \mathbf{I})^{-1} \mathfrak{g}^T (Q - \Theta) . \quad (13)$$

The algorithm used to choose the damping value μ_n is described in detail by Marquardt [12].

The bridge between the CFD code and the LMM algorithm is formed by the INPUT/OUTPUT files. The information delivered from the CFD code to the LMM algorithm is the calculated volume flow rate of air and the Jacobian matrix, and the information delivered from the LMM algorithm to the CFD code is the newly estimated shape for the centrifugal fan. These files should be arranged such that their format can be recognized by both the CFD code and the LMM algorithm. A sequence of forward centrifugal fan problem is solved by using the CFD code to update the geometry of the centrifugal fan by minimizing the residual measured differences between the estimated and desired volume flow rates of air using the present algorithm.

After the airflow rate has been obtained, the following equation can be used to calculate the efficiency of the centrifugal fan

$$\eta = \frac{P_s \times Q}{\tau \times \omega} . \quad (14)$$

Here, P_s represents the static pressure, τ represents the shear stress of the blade and ω represents the fan speed.

5. Optimization procedure

The iterative LLM computational procedure used to solve

this inverse design problem can be summarized as follows.

Choose an existing centrifugal fan to start the computation. The design variables at the zeroth iteration, B_j^0 , can be obtained from this existing centrifugal fan and are used as the starting reference variables. The desired volume flow rate of air Θ is also decided at the outset.

Step 1. Solve the direct problem using the CFD code to obtain the estimated or computed volume flow rate of air, $Q[\Psi(B_j)]$.

Step 2. Check the end criterion. If the end criterion is not satisfied, continue to Step 3; otherwise, end the iteration.

Step 3. Construct the Jacobian matrix in accordance with Eq. (12).

Step 4. Update \mathbf{B} from Eq. (13) and compute the new centrifugal fan geometry in accordance with the standard procedure set out in section 3. Iterate from step 1.

6. Statistical analysis

Statistical analysis is important in determining the estimated design variables, \mathbf{B} , by assuming independent, constant-variance errors. The variance-covariance matrix of the estimated design variables vector \mathbf{B} is defined as [19]

$$\text{Var-cov}(\mathbf{B}) \equiv E[\mathbf{B} - E(\mathbf{B})][\mathbf{B} - E(\mathbf{B})]^T \tag{15}$$

where $\mathbf{B} = \mathbf{B}(\Theta)$ is the unknown design variables vector, Θ is the desired volume flow rate of air, $E(\bullet)$ denotes the statistically expected value (averaging) operator, and the superscript T refers to the transpose matrix. Eq. (15) is a nonlinear system used to determine the variance-covariance matrix.

The right hand side of Eq. (15) is then linearized by expanding \mathbf{B} and $E(\mathbf{B})$ using a Taylor series and neglecting the higher-order terms. We thus obtain

$$\begin{aligned} \text{Var-cov}(\mathbf{B}) &= \left[\frac{\partial \mathbf{B}}{\partial \Theta^T} \right] E \left[[\Theta - E(\Theta)][\Theta - E(\Theta)]^T \right] \left[\frac{\partial \mathbf{B}^T}{\partial \Theta} \right] \end{aligned} \tag{16}$$

For independent volume flow rate measurements with constant variance σ^2 , we obtain [19]

$$E[[\Theta - E(\Theta)][\Theta - E(\Theta)]^T] = \sigma^2 \mathbf{I} \tag{17}$$

Introducing Eq. (17) into Eq. (16), the variance-covariance matrix becomes

$$\text{Var-cov}(\mathbf{B}) = \sigma^2 \left[\frac{\partial \mathbf{B}}{\partial \Theta^T} \right] \left[\frac{\partial \mathbf{B}^T}{\partial \Theta} \right] \tag{18}$$

To express the right-hand side of Eq. (18) in terms of a Jacobian, the chain-rule method is applied and the high-order terms are neglected. After lengthy manipulations, the follow-

ing equation is obtained:

$$\text{Var-cov}(\mathbf{B}) = \sigma^2 \left\{ \left[\frac{\partial Q^T}{\partial \mathbf{B}} \right] \left[\frac{\partial Q}{\partial \mathbf{B}^T} \right] \right\}^{-1} \tag{19}$$

If independent errors are assumed, the non-diagonal elements in the variance-covariance matrix vanish, and the matrix can be written in an explicit form as

$$\text{Var-cov}(\mathbf{B}) = \begin{bmatrix} \sigma_{B_1}^2 & 0 & \dots & 0 \\ 0 & \sigma_{B_2}^2 & & \vdots \\ \vdots & & \ddots & 0 \\ 0 & \dots & 0 & \sigma_{B_p}^2 \end{bmatrix} \tag{20}$$

Comparison of Eqs. (19) and (20) yields the standard deviation of the estimated parameters σ_B as

$$\sigma_B = \sigma \sqrt{\text{diag} \left\{ \left[\frac{\partial Q^T}{\partial \mathbf{B}} \right] \left[\frac{\partial Q}{\partial \mathbf{B}^T} \right] \right\}^{-1}} \tag{21}$$

where σ is the standard deviation of the measurements of the air volume flow rate. This result is identical to that obtained by Maniatty and Zabarar [20]. Based on Eq. (21), if the measurement error is assumed to follow a normal distribution, then intuitively the estimates are also normally distributed.

Once the estimated design variables have been obtained by using the standard derivation, some confidence bounds will naturally be of interest. For this reason, Flach and Ozisik [21] proposed that the confidence bounds equation be used for the estimated quantities.

If we now assume that the measurement errors are normally distributed, the 99% confidence bounds can be determined by [21]

$$\{\mathbf{B} - 2.576\sigma_B \leq \mathbf{B}_{mean} \leq \mathbf{B} + 2.576\sigma_B\} = 99\% \tag{22}$$

This expression defines the approximate statistical confidence bounds for the estimated design variables vector \mathbf{B} , i.e., the estimated values of the design variables are expected to lie between these two bounds with 99% confidence.

7. Experiments for centrifugal fan performance testing

A centrifugal fan performance test was conducted with the original and optimal fans according to the AMCA 210-85 guideline [22]. This AMCA standard defines uniform methods for conducting laboratory tests on housed fans to determine airflow rate, pressure, power and efficiency, at a given speed of rotation. The experiment is conducted using type-200 and type-400 inlet chambers; the type-200 chamber is used to

measure the airflow rate, and the type 400-chamber is used to measure the static pressure. The air volume flow rate was measured using a Yokogawa WT1600 power meter with an accuracy rating of $\pm 0.1\%$. The purpose of these experiments is to test the accuracy of the CFD code, i.e., to show that the numerical and experimental airflow rates are consistent under the specified operational and geometrical conditions.

The experimental measurement of fan noise was conducted in a hemi-anechoic chamber. The inside surfaces are completely lined with mineral wool wedges that are 59 cm deep, as this material has good absorption characteristics at frequencies greater than 150 Hz. A TES-1357 sound level meter is used to measure fan noise at 0.1 dB resolution with a fast/slow dynamic characteristic and A&C frequency weighting. The measurement range is from 10 to 130 dB. This experiment is used to measure the noise from fabricated original and optimized centrifugal fans.

8. Results and discussion

Due to the low-velocity characteristics of centrifugal fans, an NACA4412 [23] wing section is chosen as the basic rotor blade shape to achieve high fan performance. The system variables for the original centrifugal fan are shown in Table 1, and the shape of the corresponding centrifugal fan can be constructed using the technique stated in section 3, FAN SHAPE GENERATION; the grid system for the fan blades and the computational domain can be obtained automatically using the CFD-ACE+ code. Fig. 3(a) shows the computational domain of the flow field, and Figs. 3(b) and 3(c) indicate the grid systems for the impeller and volute, respectively. After the centrifugal fan grid system has been obtained, the volume flow rate of air can be calculated by using the CFD-ACE+ code.

The numerical solution for the airflow rate depends strongly on the number of grids in the system, particularly for complicated flow structure problems such as this. For this reason, the grid-independent test must be examined. In the present study, the four grid numbers 466,908, 579,314, 694,860 and 753,176 were tested to calculate the air volume flow rates, and the results obtained were 2.1332 CFM, 2.9491 CFM, 3.8833 CFM and 3.8806 CFM, respectively. The computer time used for grid numbers 466,908; 579,314; 694,860 and 753,176 was obtained as 437, 521, 630 and 745 minutes, respectively. From these results, it is apparent that for grid numbers beyond 694,860, the change in airflow rate is small; therefore, the grid number 694,860 is used for all calculations in the present work.

By performing a sensitivity analysis for the design variables as mentioned in section 4, the changes in the volume flow rate of air can be determined (Table 2). Based on the values listed in the table, it can be concluded that when using the same scale of perturbation for each variable, the changes are prominent only for the four variables m , β , R_i and R_h . However, R_h depends on the size of the motor and cannot be changed arbitrarily. This implies that only three variables are sensitive to

Table 1. The system variables for the various fan blades considered in this work.

	Original fan	Optimal fan	Tested fan #1	Tested fan #2	Tested fan #3
NACA airfoil (m, p, ta)	4412	6412	<u>7412</u>	6412	6412
Inner radius of the impeller (r_1, mm)	14	14	14	14	14
Outer radius of the impeller (r_2, mm)	20	20	20	20	20
Width of the impeller (h, mm)	8	8	8	8	8
Radius of the rotor (R_h, mm)	11	11	11	11	11
Blade inlet angle ($\beta, degree$)	31	23.2	23.2	<u>22.0</u>	23.2
Number of blades (N)	23	23	23	23	23
Inclined angle of the volute tongue ($\theta, degree$)	45	45	45	45	45
Impeller blade-tongue clearance ($\Delta r, mm$)	2.4	2.4	2.4	2.4	2.4
Radius of the inlet flow (R_i, mm)	15.5	18.3	18.3	18.3	<u>19.0</u>
Fan speed (ω, rpm)	3,600	3,600	3,600	3,600	3,600
Calculated air volume flow rate (Q, CFM)	3.8833	4.4119	4.4101	4.4107	4.3096
Measured air volume flow rate (Q, CFM)	3.6214	4.0491	N/A	N/A	N/A
Measured fan noise (FN, dB)	31.2	30.1	N/A	N/A	N/A

the volume flow rate of air; therefore, these three variables are chosen as the key design variables in the present study:

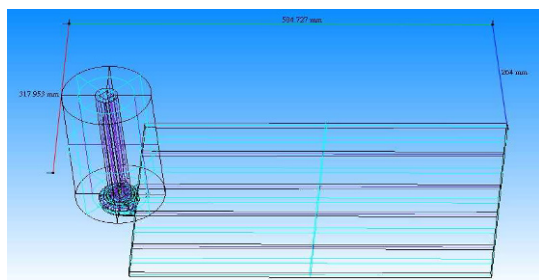
$$B = \{B_1, B_2, B_3\} = \{m, \beta, R_i\}. \quad (23)$$

The remaining system parameters are kept constant during the entire calculation. Using these three design variables, the following centrifugal fan shape design problem can be solved.

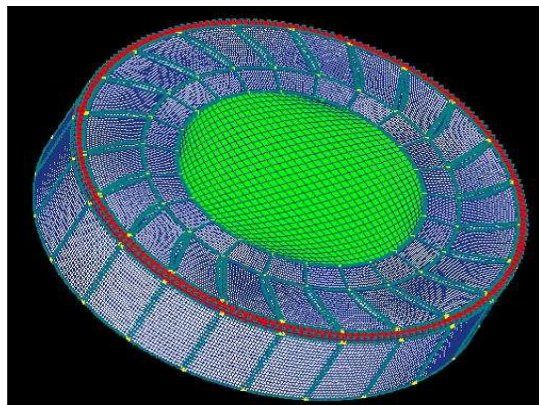
In the fan shape design optimization problem, a large number is assigned to the desired volume flow rate of air Θ at $P_s = 0$, and the LMM algorithm is used to obtain the optimal fan shape that meets the requirements as closely as possible. The

Table 2. Sensitivity analysis of the design variables.

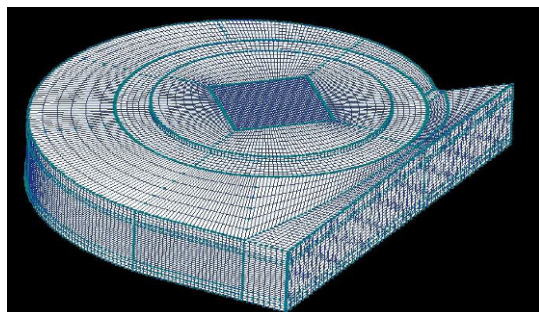
Variable	Perturbed condition	Resultant CFM	Percentage change in CFM
$\beta = 31.0^\circ$	$32.55^\circ (+5\%)$	3.83	-1.31%
$\beta = 31.0^\circ$	$29.45^\circ (-5\%)$	4.01	+3.21%
$R_i = 15.5 \text{ mm}$	$16.28 \text{ mm} (+5\%)$	3.97	+2.12%
$R_i = 15.5 \text{ mm}$	$14.73 \text{ mm} (-5\%)$	3.88	-0.89%
$R_h = 11.0 \text{ mm}$	$11.55 \text{ mm} (+5\%)$	3.77	-2.81%
$R_h = 11.0 \text{ mm}$	$10.45 \text{ mm} (-5\%)$	3.88	-0.11%
NACA4412	NACA 5412 (m+1)	3.93	+1.28%
NACA4412	NACA 3412 (m-1)	3.80	-2.06%
NACA4412	NACA 4512 (p+1)	3.87	-0.38%
NACA4412	NACA 4312 (p-1)	3.89	+0.21%
NACA4412	NACA 4413 (ta+1)	3.86	-0.65%
NACA4412	NACA 4411 (ta-1)	3.86	-0.71%



(a)

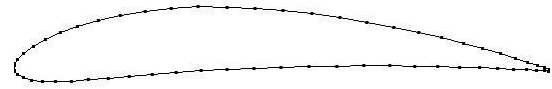
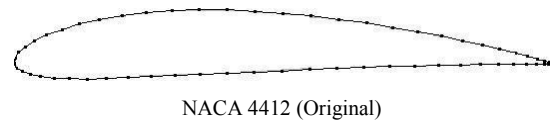


(b)

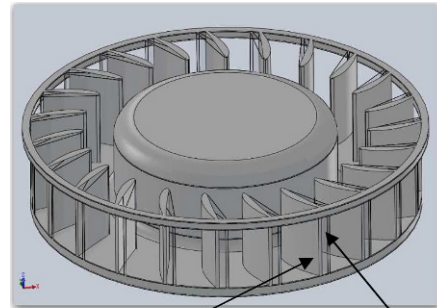


(c)

Fig. 3. The (a) computational domain of flow field and the grid systems; (b) an impeller; (c) a volute.



(a)



(b)

Fig. 4. (a) Cross-sectional views for NACA 4412 and NACA 6412; (b) Original and optimal blade inlet angles.

objective function cannot be reduced to a small number in this case; however, the optimal shape for the centrifugal fan can still be obtained.

By requiring an increase of 20 % in the volume flow rate of air at $P_s = 0$, i.e., setting $\Theta = 4.6599 \text{ CFM}$ at $P_s = 0$ and using the system variables for the original fan as the initial guesses for the design variables. After seven iterations, the design variables of $\{m, \beta, R_i\}$ for the estimated optimal centrifugal fan can be obtained (Table 1). Table 1 shows that the volume flow rate of air for the optimal fan blade is just 4.4119 CFM at $P_s = 0$, i.e., the airflow rate is increased by only 13.6%. This implies that an increase in airflow rate of 20 % rate cannot be reached; nevertheless, the optimal improvement in airflow rate can still be obtained. Fig. 4(a) shows cross-sectional views for NACA 4412 and NACA 6412, and Fig. 4(b) compares the original and optimal blade inlet angles.

Next, it is of interest to examine why the newly estimated fan shape performs better at producing higher volume flow rates of air than the existing fan shape. To study this, it is necessary to analyze the visualized pressure distributions and the flow patterns inside the volute using numerical techniques. Figs. 5(a) and 5(b) show the pressure distributions of the original and optimized centrifugal fans, respectively, on the plan at $z = 10 \text{ mm}$. It is obvious from the circles that are marked in Fig. 5 that a larger pressure drop exists around the original fan blade than around the optimized fan blade. As a result, severe reverse flow (or back flow) occurs between the blades in the original fan; therefore, the total airflow rate decreases, and the noise increases.

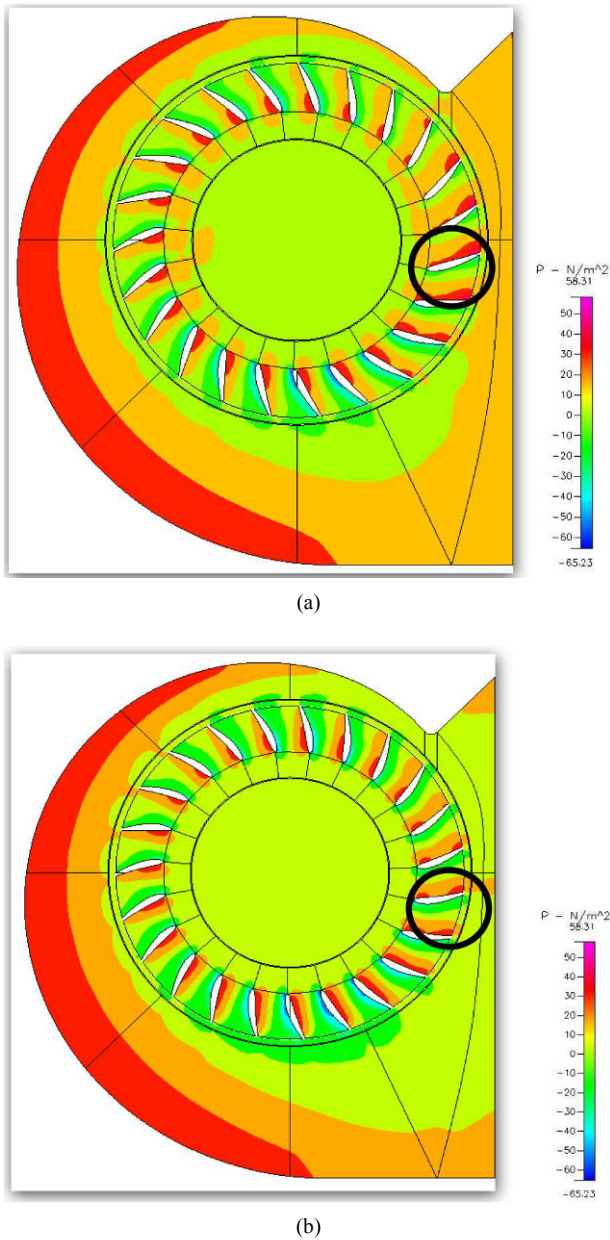


Fig. 5. The pressure distribution: (a) original; (b) optimal.

This phenomena can be visualized from the flow distributions obtained using the direct problem calculations. Visualization of the flow is extremely difficult using experimental techniques, but is essential for understanding complicated flow phenomena within small centrifugal fans. Figs. 6(a) and 6(b) show the flow patterns between the original fan blades in the impeller and the optimized fan blades, respectively. It is obvious from the circles that are marked in Figs. 6(a) and 6(b) that the reverse flow in the original fan is more severe than that in the optimized fan, and therefore, the airflow rate in the optimized fan is greater.

The estimated results also show that when m and R_i are increased and β is decreased, the total volume flow rate of air for the estimated optimal centrifugal fan can be increased for

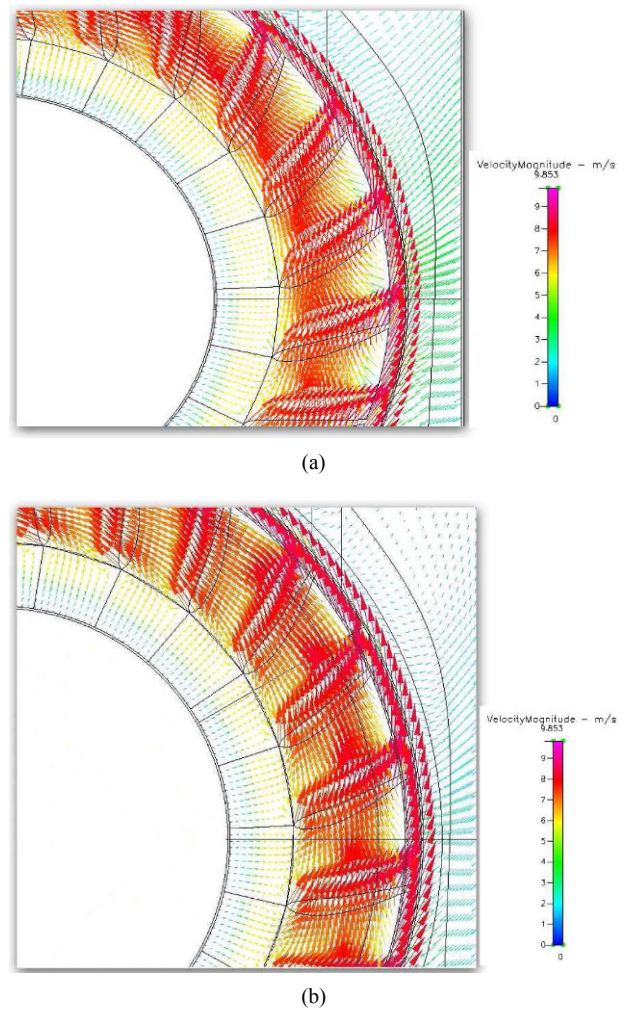


Fig. 6. The reverse flow distributions between fan blades in the impeller: (a) original; (b) optimal fans at $z = 10$ mm.

the reasons stated above. The question now arises whether the performance of the centrifugal fan can be improved further if we continue increasing the value of m and R_i or decreasing the value of β . If the answer is yes, then the current fan design is not optimal!

To answer this question, the following three computations are required. First, the value for m is increased from the optimal value of 6 to 7 while the optimal values of R_i and β are held constant; then, the total volume flow rate of air for this tested fan#1 is computed. The value for β is then decreased from the optimal value of 23.2° to 22° , the optimal values of m and R_i are held constant and the total volume flow rate of air for tested fan#2 is computed. Finally, the value for R_i is increased from the optimal value of 18.3 mm to 19 mm while the optimal values of m and β are held constant, and the total air volume flow rate for tested fan#3 is computed.

The total volume flow rates of air computed for these three cases are listed in Table 1. It is obvious that the three air flow rates generated by the three tested fans are less than the rate generated by the optimized fan. This confirms that the optimal

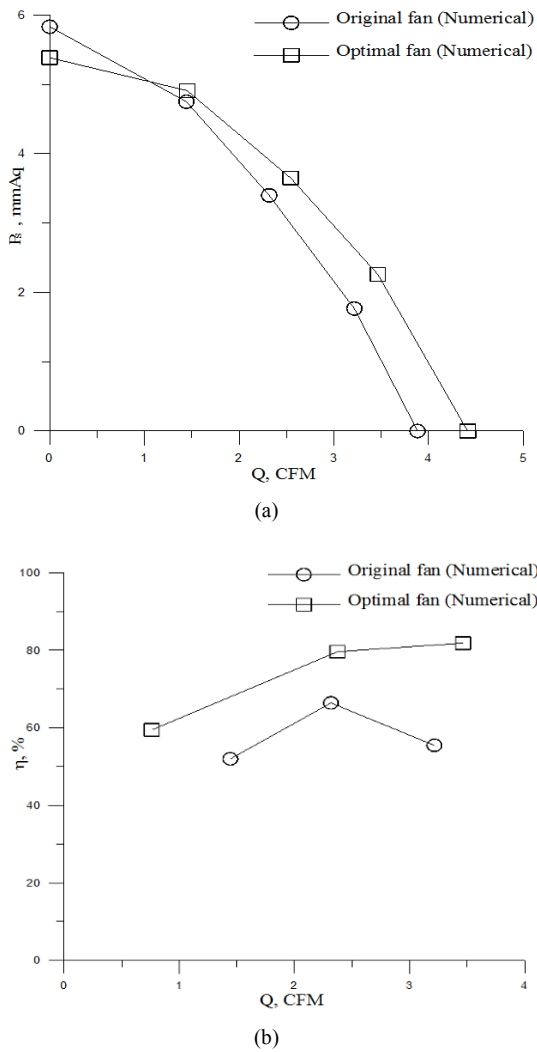


Fig. 7. Numerical solutions of original and optimal fans: (a) P_s - Q ; (b) η - Q curves.

centrifugal fan design is indeed the optimal one.

The numerical solutions for the original and optimized fans are compared in Figs. 7(a) and 7(b), respectively, using P_s - Q and η - Q curves. It can be seen from both figures that the optimal fan design performs better than the original fan because it has a higher airflow rate for the same static pressure and a higher fan efficiency for the same airflow rate.

As mentioned previously, statistical analysis is important in determining the reliability of the estimated design variables. For this reason, the 99% confidence bounds for the estimated variables must be calculated. For the optimal fan, the airflow rate is calculated to be $0.00242 \text{ m}^3/\text{s}$. Assuming the standard deviation of the airflow measurement is 10 % of the airflow rate, a value of $\sigma = 0.000242$ can be used to calculate the standard deviation of the design variables and the 99% confidence bounds.

The calculated standard deviations of the design variables and 99% confidence bounds are shown in Table 3. It can be

Table 3. The estimated standard deviation and 99 % confidence bounds for the design variables for an optimal fan blade with $\sigma = 0.000242$.

	β	R_i	m
σ_B	0.00006	0.00018	0.00027
$B_{\text{mean}} - 2.576\sigma_B$	23.1998	18.2995	5.9993
B_{mean}	23.2	18.3	6
$B_{\text{mean}} + 2.576\sigma_B$	23.2002	18.3005	6.0007

seen from Table 3 that with 10 % measurement error in the airflow rate, the estimated standard deviations of the design variables are very small; therefore, the band of the 99% confidence bounds becomes very narrow. This implies that the present design algorithm is reliable because most of the designs are within these narrow bounds.

The accuracy of the solution provided by the CFD code for the flow field fan calculations plays an important role in the present centrifugal fan design problem. If the solution provided by the CFD code cannot reproduce the actual performance of the fan, the design will never be obtained accurately. The first task is therefore to demonstrate the validity of the numerical solution for the airflow rate provided by the CFD code by comparing it with the experimental data. The benchmark problem for the numerical solution for the airflow rate of fans provided by the CFD code must be examined here based on the experiments conducted in this work for the original and optimal centrifugal fans.

For this reason, the original and optimized centrifugal fans must be CNC fabricated in accordance with the fan design variables. The numerical data for fan shapes obtained from the CFD code can be used in a CNC machine to fabricate the fan shapes for use in experiments. Figs. 8(a)-8(c) illustrate the volute cover with a driving motor, the original impeller and the optimal impeller, respectively, as fabricated using a CNC machine.

The experimental apparatus used for AMCA 210-85 with 200-type and 400-type inlet chambers and the corresponding data acquisition panel are illustrated in Figs. 9(a) and 9(b), respectively, and the operational conditions for the centrifugal fan have been described in the preceding section. Figs. 10(a) and 10(b) compare the experimental results for the original and optimal fans using P_s - Q and η - Q curves, respectively. Based on Fig. 10, it is clear that the experiments performed quite well because the trend of the P_s - Q and η - Q curves for both centrifugal fans is also reasonable. More importantly, the optimal fan indeed performs better than the original fan, and this also demonstrates the validity of the present optimal design.

It can be seen from Fig. 10(a) that at the design point ($P_s = 0$), the airflow rates for the original and optimal fans are 3.6214 CFM and 4.0491 CFM, respectively. This implies that the airflow rate has been increased by 11.8%. Although the numerical simulations predict that the airflow of the optimal



(a)



(b)



(c)

Fig. 8. The CNC machine-fabricated: (a) volute cover and driving motor; (b) original impeller; (c) optimal impeller.

fan is 13.6% greater than that of the original fan, the design remains effective because the 11.8% increase is quite significant. From Fig. 10(b), it is clear that the efficiency of the optimal fan is always higher than that of the original fan. From Figs. 10(a) and 10(b), it is evident that the redesigned optimal centrifugal fan performs better than the original fan.

The final task is to compare the numerical results with the experimental results for the original and optimal fans. The



(a)



(b)

Fig. 9. The experimental apparatus: (a) AMCA 210-99 200-type and 400-type wind tunnels; (b) the data acquisition panel.

purpose of this comparison is to verify the accuracy of the optimal numerical design of the centrifugal fan. Figs. 11(a) and 11(b) compare the numerical and experimental results using P_s - Q curves for the original and optimal fans, respectively. At the design point $P_s = 0$, the numerical and experimental airflow rates of the original fan blade are 3.8833 CFM and 3.6214 CFM, respectively, i.e., the discrepancy is 6.74%. The results for the optimal fan are 4.4119 CFM and 4.0491 CFM, respectively, i.e., the discrepancy is 8.22%. Therefore, it can be concluded that the numerical solutions for the fan shape design problem presented here are reliable, and the design of the centrifugal fan is practical.

Finally, noise measurements for the original and optimal centrifugal fans are conducted in a hemi-anechoic chamber. Fig. 12(a) presents an overview of the hemi-anechoic chamber, and Fig. 12(b) illustrates a TES-1357 Sound Level Meter. The background noise is measured at 17.5 dB, and the noise of the original and optimal fans is measured at 31.2 dB and 30.1 dB, respectively. The noise of the fan is reduced by 3.5%, representing a great improvement. The major cause of this improvement is that the reverse flow in the optimal fan near the blade tip region is greatly decreased. This might not only increase the airflow rate but also reduce the noise.

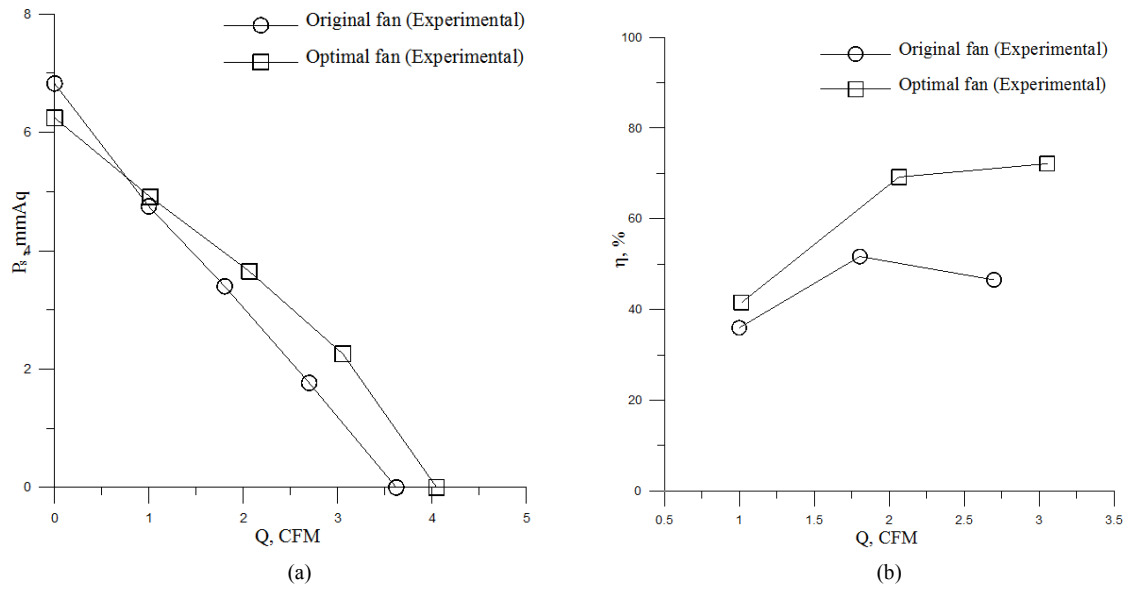


Fig. 10. The experimental results for the original and optimal fans: (a) P_s - Q ; (b) η - Q curves.

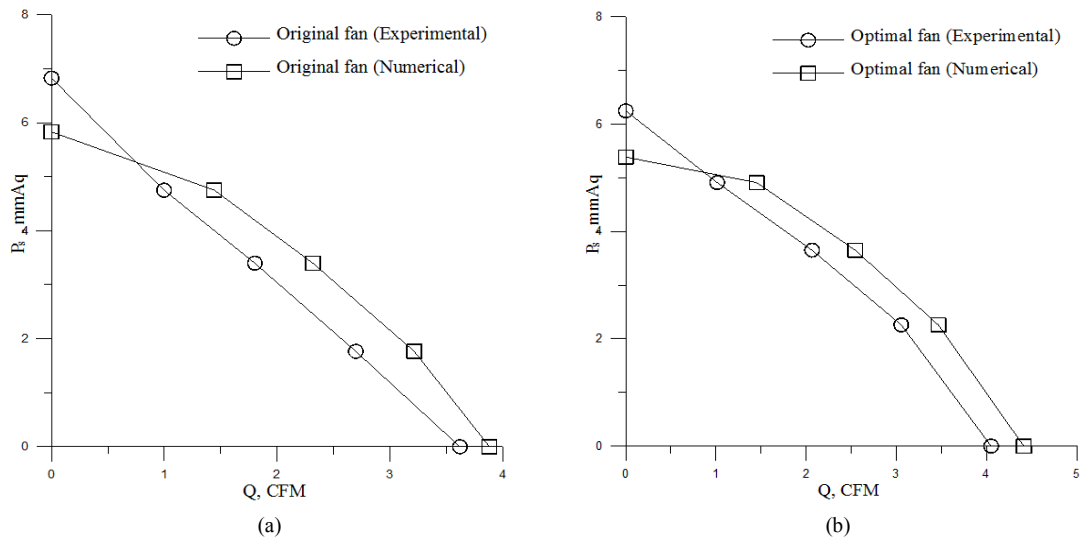


Fig. 11. Numerical and experimental results: the P_s - Q curve for (a) original; (b) optimal fans.



Fig. 12. (a) The hemi-anechoic chamber; (b) the TES-1357 sound level meter and centrifugal fan.

9. Conclusions

We successfully examined the centrifugal fan shape design problem of estimating the optimal shape of a centrifugal-flow fan based on a knowledge of the desired volume flow rate of air using commercial CFD-ACE+ code and the Levenberg-Marquardt method. Numerical calculations were first performed to design the optimal shape of the centrifugal fan. Then, experiments were conducted to verify the accuracy of and validate the estimations. The results demonstrate that the algorithm requires only a few iterations to obtain the optimal fan shape, and the volume flow rate of air and the fan efficiency can both be increased while the noise is reduced in the resulting optimal fan.

The advantages of using the present technique to design the optimal shape of a centrifugal fan are (1) the time needed for the blade redesign can be shortened, and (2) an experienced designer is not required to design the fan shape: any beginner can easily accomplish the task.

Acknowledgment

This work was supported in part through the National Science Council, R. O. C., Grant number NSC-100-2221-E-006-011-MY3.

Nomenclature

B_j	: Design variables
$E(\bullet)$: The expected value
h	: Width of the impeller
J	: Functional defined by Eq. (5)
m	: Blade section parameter
N	: Number of blades
p	: Blade section parameter
p_s	: Static pressure
Q	: Calculated air flow rate
r_1	: Inner radius of the impeller
r_2	: Outer radius of the impeller
R_h	: Radius of the rotor
R_i	: Radius of the inlet flow
ta	: Blade section parameter
u_i	: Flow velocity

Greek letters

β	: Blade inlet angle
Δr	: Impeller blade-tongue clearance
\mathfrak{J}	: Jacobian matrix defined by Eq. (12)
Ψ	: Fan domain
μ^n	: Damping parameter
η	: Fan efficiency
ω	: Fan speed
θ	: Inclined angle of the volute tongue
Θ	: Desired airflow rate

τ	: Shear stress of the fan blades
σ	: Standard deviation

References

- [1] W. N. Dawes, P. C. Dhanasekaran, A. A. J. Demargne, W. P. Kellar and A. M. Savill, Reducing Bottlenecks in the CAD-to-Mesh-to-Solution Cycle Time to Allow CFD to Participate in Design, *ASME Journal of Turbomachinery*, 123 (3) (2001) 552-557.
- [2] M. Zangeneh, Inviscid-viscous interaction method for 3d inverse design of centrifugal impellers, *ASME Journal of Turbomachinery*, 116 (1994) 280-290.
- [3] A. Demeulenaere and R. Van den Braembussche, Three-dimensional inverse method for turbomachinery blading design, *ASME Journal of Turbomachinery*, 120 (2) (1998) 247-255.
- [4] J. S. Kim and W. G. Park, Optimized inverse design method for pump impeller, *Mechanics Research Communications*, 27 (2000) 465-473.
- [5] C. K. Huang and M. E. Hsieh, Performance analysis and optimized design of backward-curved airfoil centrifugal blowers, *HVAC&R RESEARCH*, 15 (3) (2009) 461-488.
- [6] A. Behzadmehr, Y. Mercadier and N. Galanis, Sensitivity analysis of entrance design parameters of a backward-inclined centrifugal fan using DOE method and CFD calculations, *Journal of Fluids Engineering-Transactions of the ASME*, 128 (3) (2006) 446-453.
- [7] E. B. Gardow, On the relationship between impeller exit velocity distribution and blade channel flow in a centrifugal fan, *Ph.D. Thesis*, State University of New York at Buffalo (1968).
- [8] J. H. Zhou and C. X. Yang, Parametric design and numerical simulation of the axial-flow fan for electronic devices, *IEEE Transactions on Components and Packaging Technologies*, 33 (2) (2010) 287-298.
- [9] S. C. Lin and C. L. Huang, The study of a small centrifugal fan for a notebook computer, *The 8th International Symposium on Transport Phenomena and Dynamics of Rotating Machinery*, Honolulu, Hawaii, USA, (2000) 247-256.
- [10] CFD-ACE+ user's manual, 2005, ESI-CFD Inc.
- [11] J. S. Arora, *Introduction to Optimum Design*, McGraw-Hill Book Company, New York (1989).
- [12] D. M. Marquardt, An algorithm for least-squares estimation of nonlinear parameters, *J. Soc. Indust. Appl. Math.*, 11 (2) (1963) 431-441.
- [13] C. H. Huang, C. C. Chiang and S. K. Chou, An inverse geometry design problem in optimizing the hull surfaces, *Journal of Ship Research*, 42 (2) (1998) 79-85.
- [14] P. F. Chen and C. H. Huang, An inverse hull design approach in minimizing the ship wave, *Ocean Engineering*, 31 (13) (2004) 1683-1712.
- [15] P. F. Chen, C. H. Huang, M. C. Fang and J. H. Chou, An inverse design approach in determining the optimal shape of bulbous bow with experimental verification, *Journal of Ship*

Research, 50 (1) (2006) 1-14.

- [16] C. H. Huang, L. Y. Chen and S. Kim, An inverse geometry design problem in optimizing the shape of gas channel for proton exchange membrane fuel cell, *J. Power Sources*, 187 (1) (2009) 136-147.
- [17] C. H. Huang and J. W. Lin, Optimal gas channel shape design for a serpentine PEMFC – Theoretical and Experimental Studies, *J. Electrochemical Society*, 156 (1) (2009) B178-187.
- [18] L. Zhang, S. L. Wang, D. F. Wu and Q. Zhang, Numerical study for centrifugal fan based on parametric method, *Applied Mechanics and Materials*, 55-57 (2011) 892-897.
- [19] R. W. Farebrother, *Linear least square computations*, Marcel Dekker, Inc., New York (1988).
- [20] A. M. Maniatty and N. J. Zabaras, Investigation of regularization parameters and error estimating in inverse elasticity problems, *Int. J. Numer. Methods Engineering*, 37 (6) (1994) 1039-1052.
- [21] G. P. Flach and M. N. Ozisik, Inverse heat conduction problem of simultaneously estimating spatially varying thermal conductivity and heat capacity per unit volume, *Numerical Heat Transfer*, 16 (2) (1989) 249-266.
- [22] *Laboratory method of testing fans rating*, American National Standard, Air Movement and Control Association, Inc., Publication 210 (1985).
- [23] S. C. Lin and C. L. Huang, An integrated experimental and

numerical study of forward-curved centrifugal fan, *Experimental Thermal and Fluid Science*, 26 (5) (2002) 421-434.



Cheng-Hung Huang received the B.Sc. degree from National Cheng Kung University, Tainan, Taiwan, in 1983, and the M.Sc. and Ph.D. degrees from the North Carolina State University, Raleigh, NC, USA, in 1991, all in Mechanical Engineering. In 1991, he joined the faculty of the Department of Systems and Naval

Mechatronic Engineering, National Cheng Kung University, Tainan, Taiwan, where he is currently a professor. His research interests include inverse problems, system design problems and system identification problems.



Min-Hsiang Hung received the B.Sc. degree from National Taipei University of Technology in Energy and Refrigerating Air-Conditioning Engineering department and M.S. from National Cheng Kung University in Systems and Naval Mechatronic Engineering department, in 2008 and 2011, respectively.